Bioelectrochemistry 140 (2021) 107750

Contents lists available at ScienceDirect

Bioelectrochemistry

journal homepage: www.elsevier.com/locate/bioelechem

Optimizing the electrical conductivity of polyacrylonitrile/polyaniline with nickel nanoparticles for the enhanced electrostimulation of Schwann cells proliferation

Mayue Wang [a,b,c], Pier-Luc Tremblay [a,b,*], Tian Zhang [a,b,c,d,*]

[a] School of Chemistry, Chemical Engineering and Life Science, Wuhan University of Technology, Wuhan 430070, PR China
[b] State Key Laboratory of Silicate Materials for Architectures, Wuhan University of Technology, Wuhan 430070, PR China
[c] School of Materials Science and Engineering, Wuhan University of Technology, Wuhan 430070, PR China
[d] Sanya Science and Education Innovation Park, Wuhan University of Technology, Sanya 572024, PR China

ARTICLE INFO

Article history:
Received 7 December 2020
Received in revised form 9 January 2021
Accepted 24 January 2021
Available online 30 January 2021

Keywords:
Nerve tissue engineering
Electrospinning
PAN/PANI
Ni nanoparticles
Schwann cells

ABSTRACT

Tissue engineering scaffolds made of biocompatible polymers are promising alternatives for nerve reparation. For this application, cell proliferation will be speeded up by electrostimulation, which required electrically-conductive materials. Here, a biomimicking scaffold with optimized conductivity was developed from electrospun polyacrylonitrile/electrically-conductive polyaniline (PAN/PANI) nanofibers doped with Ni nanoparticles. PAN/PANI/Ni was biocompatible for Schwann cells and exhibited a suitable tensile strength and wettability for cell proliferation. When compared with unmodified PAN/PANI, the electrical conductivity of PAN/PANI/Ni was 6.4 fold higher. Without electrostimulation, PAN/PANI and PAN/PANI/Ni exhibited similar Schwann cells' proliferation rates. Upon electrostimulation at 100 mV cm^{-1} for one hour per day over five days, PAN/PANI/Ni accelerated Schwann cells' proliferation 2.1 times compared to PAN/PANI. These results demonstrate the importance of expanding the electrical conductivity of the tissue engineering scaffold to ensure optimal electrostimulation of nerve cell growth. Additionally, this study describes a straightforward approach to modulate the electrical conductivity of polymeric materials *via* the addition of Ni nanoparticles that can be applied to different biomimicking scaffolds for nerve healing.

1. Introduction

Peripheral nerve tissue damage caused by physical trauma, diabetes, vascular problems, cancer, and so on, are difficult to cure and seriously affect the quality of life of patients because of high disability rates [1–4]. Multiple nerve injuries with large gap cannot be repaired by end to end sutures and require autologous nerve grafts [5,6]. However, this approach has several limitations such as partial loss of function for donors, mismatch with recipients, and shortage of donors [7]. A promising alternative being the object of vast research effort is nerve tissue engineering (NTE) where artificial biomimicking scaffolds similar to extracellular matrices can regulate, guide, and nurture cell proliferation to promote nerve reparation [8].

For NTE, electrically-conductive scaffolds such as electrospun nanofibers have been developed to promote nerve cell outgrowth [9–12]. Electrical stimulation induces particular cell responses at the molecular level leading to nerve regeneration [13–16]. Schwann cells (SC) are of distinct importance when it comes to neurite or axonal growth. They ensure the re-myelination of injured nerves, participate in the removal of myelin debris, and release soluble factors promoting re-growth [17–20]. Upon exogenous electrical stimulation, SCs were shown to proliferate, increase the release of nerve growth factors, and promote neurite regeneration [18,21,22].

Several electrically-conductive biomimicking scaffolds have been developed to stimulate SC proliferation. These include matrices made of conductive polymers such as polypyrrole (PPy) coated on indium tin oxide, interwoven PPy and poly(styrene sulfonate) on a polycaprolactone (PCL) substrate, PPy/chitosan composite, PPy coated on electrospun poly(L-lactic acid-co-e-caprolactone)/silk fibroin nanofibers, micropatterned poly(glycerol sebacate)–co-aniline pentamer, graphene/silk fibroin composite, PCL/poly

* Corresponding authors at: School of Chemistry, Chemical Engineering and Life Science, Wuhan University of Technology, Wuhan 430070, PR China.
E-mail addresses: pierluct@whut.edu.cn (P.-L. Tremblay), tzhang@whut.edu.cn (T. Zhang).

https://doi.org/10.1016/j.bioelechem.2021.107750
1567-5394/

(ethylene oxide) doped with graphene, chitosan/gelatin scaffold with incorporated polyaniline (PANI)/graphene nanocomposite, and PANI/cellulose [9,15,23–30]. Among these materials, PANI is a promising organic conductive polymer for tissue engineering involving electrical stimulation [31–35]. PANI has a wide electrical conductivity range that can be modulated by combining it with other conductive nanomaterials such as graphene and nickel [36–40]. Furthermore, PANI is easy to synthesize and has a good chemical stability [41].

Electrospinning is an efficient method for the fabrication of artificial biomimicking scaffold for tissue engineering [42–45]. This technique allows the preparation of highly porous mesh made of continuous nanofibers with good surface area to volume ratio, which maximizes contact with living cells [25,46]. One disadvantage of conductive PANI nanofibers is their weak mechanical strength hampering the electrospinning process [47]. A simple solution is to combine PANI with a second polymer with high mechanical strength such as polyacrylonitrile (PAN) [48,49]. PAN also has high thermal and chemical resistance as well as low cost. PAN/PANI films generated by electrospinning are stable with good mechanical strength and electrical conductivity [50]. This material has been used alone or in combination with other compounds for diverse applications such as tissue engineering, water treatment, as a supercapacitor, sensor, catalyst, and so on [33,51–55].

In this study, PAN/PANI nanofibers doped with Ni nanoparticles (NP) were synthesized. Ni NPs were selected for the modification of a PAN/PANI biomimicking scaffold primarily because of their high electrical conductivity that may enhance NTE via electrostimulation. Furthermore, Ni-based materials are earth-abundant, low-cost, antibacterial, and can be biocompatible with animal cell lines [56,57]. After physicochemical characterization, both electrospun PAN/PANI and PAN/PANI/Ni with enhanced electrical conductivity were evaluated as scaffolds for the acceleration of the proliferation of SCs involved in peripheral nerve repair [58].

2. Experimental section

2.1. Materials

PAN (Mw: 150000 g mol^{-1}) and electrically-conductive PANI doped with 5-sulfosalicylic acid (SSA) were purchased from Shanghai Macklin Biochemical (Shanghai, China). Ni NPs were acquired from Nangong Xindun Alloy Welding Material Spraying Co. (Xingtai, China). N,N-dimethylformamide (DMF) (purity $\geq$ 99.5%) was purchased from Sinopharm Chemical Reagent (Shanghai, China). DMEM cell culture medium, fetal bovine serum (FBS), penicillin–streptomycin-neomycin antibiotic mixture, and (3-(4,5-Dimethyl thiazol-2-yl)-2,5-Diphenyltetrazolium Bromide) (MTT) were acquired from ThermoFisher Scientific (Waltham, MA, USA). DMSO (purity $\geq$ 99.5%) was obtained from neoFroxx (Hessen, Germany). The cell counting kit 8 (CCK-8) was purchased from Dojindo Molecular Technologies (Rockville, MD, USA). SCs RSC96 were obtained from the China Center for Type Culture Collection (Wuhan, China).

2.2. Preparation of electrospun nanofiber films

For PAN electrospun nanofibers, 5 ml DMF was added to 0.4 g PAN. For both PAN/PANI and PAN/PANI/Ni, 0.6 g PANI was added to the PAN-DMF mixture. For PAN/PANI/Ni, 50 mg Ni NPs were added to PAN/PANI-DMF. These solutions were stirred overnight prior to being placed in an ultrasonic bath for one hour. For electrospinning, the solutions were loaded in a 5 ml syringe with a 21-gauge needle, which was placed into a syringe pump. The syringe device was then connected to a high voltage supply and the electrospinning process was conducted at a voltage of 18 kV and a flow rate of 4.2 ml h^{-1}. 15 cm separated the needle tip from the drum collector, which was rotating at 200 rpm. After electrospinning, the nanofiber film was placed into a vacuum drying oven for 24 h to remove solvents.

2.3. Characterization of electrospun nanofiber films

Fourier transform infrared (FTIR) spectra were recorded with a Nicolet IS5 spectrometer (Thermo Fisher Scientific) in the 500–4000 cm^{-1} range at a resolution of 0.8 cm^{-1} and with a scan number of 15. X-ray diffraction (XRD) spectroscopy of the electrospun nanofiber films was performed with a D8 ADVANCE powder X-ray diffractometer (Bruker, MA, USA) in the 10 – 80° range with a scan step (0.02°) per degree of 50. Scanning electron microscopy (SEM) and energy-dispersive X-ray spectroscopy (EDS) were performed at an accelerating voltage of 5 kV with a S-4800 microscope with a magnification ranging from 5000 to 100000X (Hitachi, Tokyo, Japan). Samples for SEM were mounted onto the holder with conductive adhesive and sputter-coated with gold prior to observation. Electrical conductivities of PAN, PAN/PANI, and PAN/PANI/Ni were measured with a RTS-11 double electric four-probe tester (Guangzhou Four-Probe Electronic Technology, Guangzhou, China). Tensile strengths of the electrospun nanofiber films were measured with a HY0580 universal material testing machine. Sample width was 30 mm, gauge length was 10 mm, and number of replicates per sample was five for tensile strength measurements (Shanghai Hengyi Precision Instrument, Shanghai, China). The wettability of the materials was evaluated with a JC2000S water contact angle measurement instrument (Beijing Zhongyi Kexin Technology, Beijing, China).

2.4. Schwann cell culture maintenance

SCs were maintained in culture medium comprising 89% DMEM, 10% FBS, and 1% penicillin–streptomycin-neomycin antibiotic mixture. SCs were incubated at 37 °C with a 5% CO_2 atmosphere. The culture medium was changed every two days and cellular growth was monitored under a microscope. When the cell number increased by 80 to 90%, a subculture was started.

2.5. Cytotoxicity test

For cytotoxicity analyses, SCs were cultivated in electrospun nanofiber film extractants and cell viability was assessed with the MTT assay. Briefly, PAN, PAN/PANI, and PAN/PANI/Ni were immersed in 75% ethanol for four hours. Ethanol was then removed and the materials were sterilized further under an ultraviolet lamp for 30 min. The electrospun nanofiber films were then soaked for one day at 37 °C in cell culture medium. The volume of culture medium employed for the extraction process was one ml per six cm^2 of material surface. Subsequently, the electrospun nanofiber films were removed from the extractants, which were then filter-sterilized. For each tested material, 200 µl extractant was added to six replicate wells on a 96-well plate. The positive control of cytotoxicity was 5% DMSO while the negative control was pristine cell culture medium not exposed to electrospun nanofiber films. DMSO at a high concentration of 5% has been shown to be cytotoxic for various cell line [59,60]. SCs were then trypsinized, centrifuged, and seeded into the 96-well plate at a concentration of 5×10^3 cells per well. The well plate was then incubated at 37°C with 5% CO_2 for one day. In the next step, 20 µl of 5 mg ml^{-1} MTT was added to each well followed by four hours of incubation. The cell culture medium was discarded and 200 µl DMSO was added to each well. The plate was then shaken for 10 min prior to measurement of the optical density (OD) at 490 nm with a Multiskan Fc microplate photometer (ThermoFisher Scientific).

2.6. Electrostimulation and cell proliferation assay

For electrostimulation and cell proliferation assay, electrospun nanofiber films were placed in triplicate in the wells of a 24-well plate. Each well was then filled with 100% ethanol and incubated at room temperature overnight. 100% ethanol was aspirated and replaced by 75% ethanol followed by four hours of incubation. Subsequently, the 24-well plate with the electrospun nanofiber films was sterilized under ultraviolet light for 30 min prior to being washed three times with sterile PBS buffer. SCs were then trypsinized, centrifuged, and seeded at a planting density of 10,000 cells cm^{-2} prior to incubation in culture medium at 37 °C under a 5% CO_2 atmosphere. The electrostimulation was performed with aluminum foil electrodes connected to a constant voltage DC power supply generating a field of 100 mV cm^{-1}. Where indicated, SCs were electrostimulated for one hour each day for a total of five days. Cell proliferation was assessed with the CCK-8 kit (Dojindo Molecular Technologies). ODs were measured at 450 nm with a Multiskan Fc microplate photometer (ThermoFisher Scientific). SEM images of SCs on electrospun nanofiber films were taken with a S-4800 microscope (Hitachi) at an accelerating voltage of 5 kV.

3. Results and discussion

3.1. Fourier transform infrared spectroscopy analysis

Electrospun PAN, PAN/PANI, and PAN/PANI/Ni nanofiber films were characterized by FTIR spectroscopy (Fig. 1A). The characteristic peaks of PAN nanofibers are observed at 2242.82, 1736.06, and 1452.04 cm^{-1} for all three materials [61], The NH bending vibration and CH tensile vibration peaks belonging to PANI are detected at 1639.85 and 1291.86 cm^{-1} with both PAN/PANI and PAN/PANI/Ni confirming the loading of PANI on PAN fibers during the electrospinning process. As expected, Ni addition had no impact on the structure of the nanofibers detectable by FTIR since spectra for PAN/PANI and PAN/PANI/Ni were similar. For PAN/PANI and PAN/PANI/Ni, the reduction of the intensity of the characteristic PAN band at 2242.82 cm^{-1} attributed to nitrile stretching vibration is a clear indication of the interaction of PANI with the nitrile group of PAN [47,62].

3.2. X-ray diffraction spectroscopy analysis

The three XRD spectra of PAN, PAN/PANI, and PAN/PANI with 4.8% Ni NPs (w/w) showed a pronounced diffraction peak at 17° and a weaker diffusion diffraction peak at 29° attributed to semi-crystalline PAN (Fig. 1B) [63–65]. The strong peak at 17° is characteristic of a hexagonal crystal (100) structure [62,66]. The diffuse peak at 29° corresponds to the amorphous region of PAN. For both PAN/PANI and PAN/PANI/Ni, the diffraction peaks detected at 21° and 26° are attributed to the layered and ordered structure of the PANI polymer [67], Peaks at 45° and 53° characteristic of Ni [68] indicate that the preparation of PAN/PANI/Ni by electrospinning was successful. Results with both PAN/PANI and PAN/PANI/Ni show that the addition of PANI did not change fundamentally the crystalline plane of PAN with peaks still present at 17° and 29°. However, PANI caused a reduction of the PAN-related peak at 17° demonstrating an interaction between PAN and PANI possibly involving electrostatic interactions and hydrogen bonding [62]. For PAN/PANI/Ni, an additional peak at 21.6° could not be attributed to PAN, PANI, or Ni. This peak is probably related to the presence of a small quantity of residual DMF (JCPDS card no. 48-2096) from the synthesis process in the PAN/PANI/Ni sample tested by XRD.

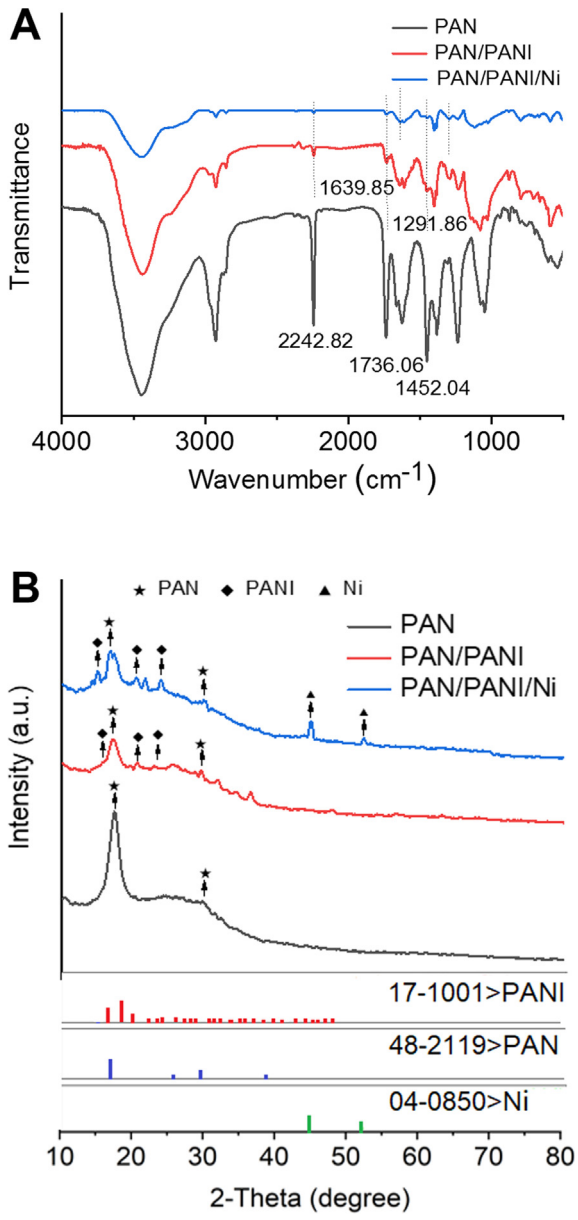

Fig. 1. Characterization of electrospun PAN/PANI/Ni nanofibers. (A) FTIR and (B) XRD spectra of PAN, PAN/PANI, and PAN/PANI/Ni. JCPDS cards no 17-1001, 48-2119, and 04-0850 correspond to PANI, PAN, and Ni, respectively.

3.3. Scanning electron microscopy and energy-dispersive X-ray spectroscopy analyses of electrospun nanofibers

The SEM image of electrospun PAN film shows a mesh of well-distributed nanofibers with an average diameter of 118.7 ± 15.4 n m (Fig. 2AB). When PANI is added, spindle-like beads are present along the nanofibers (Fig. 2C). The surface of PAN/PANI nanofibers appears to be rougher than the PAN nanofibers with a larger diameter of 190.4 ± 41.3 nm (Fig. 2D). PAN/PANI and PAN/PANI/Ni exhibit a similar appearance when observed by SEM with spindle-like structures characteristic of PANI (Fig. 2E). According to size and morphology, the inset on Fig. 2E shows a Ni NP attached to a PAN/PANI nanofiber (Fig. S1). Interestingly, PAN/PANI/Ni became narrower with a diameter of 106.6 ± 23.4 nm. This phenomenon could be attributed to the substantial electrical conductivity of Ni NPs that should lead to an increase of the electrical conductivity of the PAN/PANI/Ni solution prepared for electrospinning. During

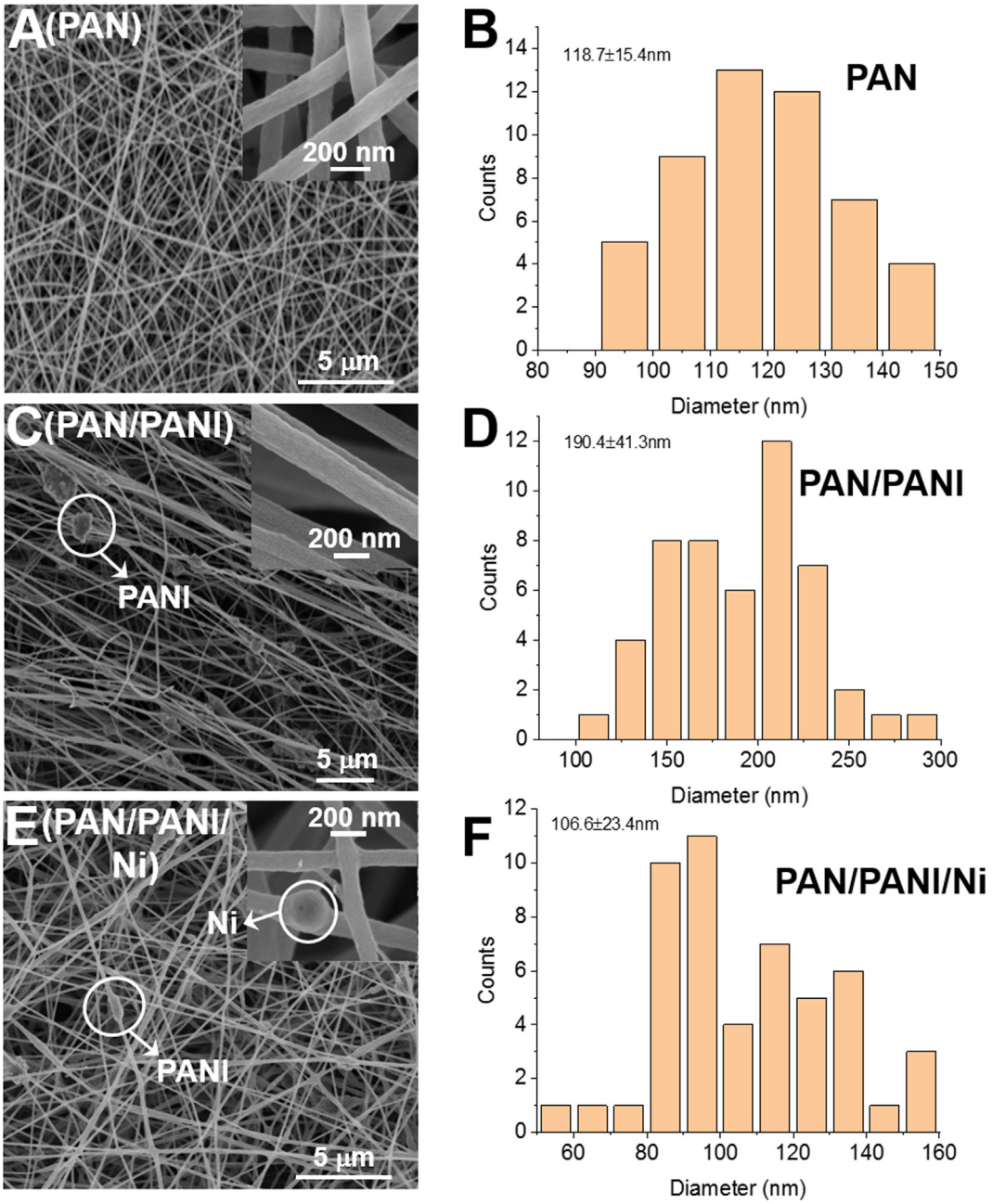

Fig. 2. SEM images of PAN, PAN/PANI, and PAN/PANI/Ni. (A) SEM images and (B) nanofiber diameter of PAN. (C) SEM images and (D) nanofiber diameter of PAN/PANI. (E) SEM images and (F) nanofiber diameter of PAN/PANI/Ni.

this process, higher electrical conductivity can lead to the fabrication of electrospun nanofiber with a smaller diameter [69,70]. For PAN/PANI/Ni, EDS analysis confirmed the successful loading of Ni NPs (Fig. 3). No Ni element was detected for PAN/PANI while the exact Ni content for PAN/PANI/Ni was 4.76% (w/w). The S element detected by EDS in both PAN/PANI and PAN/PANI/Ni is comprised in the SSA employed by the manufacturer to dope PANI.

3.4. Electrical conductivity of PAN/PANI nanofibers with nickel nanoparticles

PAN nanofiber networks such as the one fabricated here are insulators with an electrical conductivity below the detection limit of 0.01 mS cm^{-2} of the double electrical measurement 4-point probe tester employed here (Fig. 4). Adding the electrically-conductive polymer PANI to PAN increased electrical conductivity to 7.3 ± 1.2 mS cm^{-1}. When PAN/PANI nanofibers were modified with Ni NPs, electrical conductivity was further augmented by 6.4 fold to 47.0 ± 1.0 mS cm^{-1}. This is expected since pure nickel has an outstanding electrical conductivity of 1.4×10^7 S cm^{-1}. Both PAN/PANI and PAN/PANI/Ni electrospun nanofiber films cover a wide range of electrical conductivity and thus, can be used to assess the impact of this fundamental property on the electrostimulation of SC proliferation.

3.5. Tensile strength and wettability

The tensile strength of PAN, PAN/PANI, and PAN/PANI/Ni was measured to establish if these scaffold materials for cell proliferation could withstand stresses during nerve healing and maintain

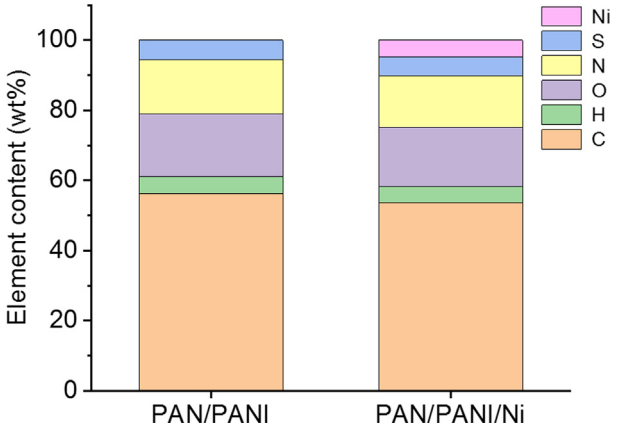

Fig. 3. Element content of PAN/PANI and PAN/PANI/Ni measured by EDS.

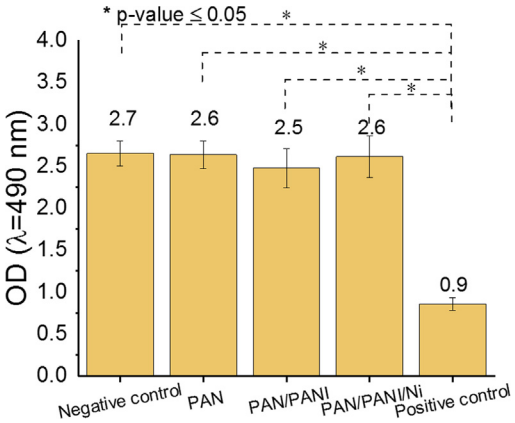

Fig. 6. Cytotoxicity of electrospun nanofiber films. Cell viability after one-day exposure to cell culture medium extractant from PAN, PAN/PANI, and PAN/PANI/Ni measured with MTT. Each bar is the mean of at least six replicates with standard deviation.

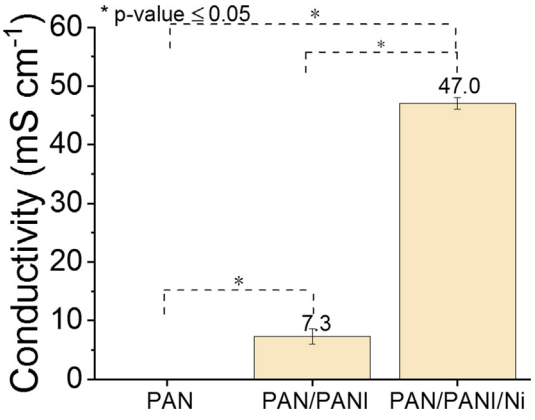

Fig. 4. Electrical conductivity of electrospun nanofiber films. Each bar is the mean of at least three replicates with standard deviation.

their shape and structural integrity [71–73]. Decellularized rat nerves have a maximum tensile strength of 1.4 MPa and it is assumed that biomimicking scaffolds for nerve healing should be in the same range [73]. The tensile strength of the PAN, PAN/PANI, and PAN/PANI/Ni nanofiber films were 3.6 ± 0.2 MPa, 2.9 ± 0.2 MPa, and 2.7 ± 0.3 MPa (n = 5), respectively (Fig. 5A). The lower tensile strength of both PAN/PANI and PAN/PANI/Ni compared to pristine PAN is probably related to the lower mechanical strength of PANI affecting the properties of the electrospun nanofiber films [47].

Still, all three materials had a comparable but slightly superior tensile strength versus decellularized rat nerves with PAN/PANI/Ni being the closest.

Another important characteristic of biomimicking scaffolds is surface wettability. Hydrophilic materials are more suitable for cell adhesion and proliferation [74,75]. This is also the case for nerve healing and SCs where hydrophilicity is an important feature of the scaffold for the maximization of cellular proliferation [26,76]. PAN exhibited a water contact angle of 125° and was hydrophobic (Fig. 5B). On the contrary, PAN/PANI and PAN/PANI/Ni were super-hydrophilic with fast permeation of the water droplet on the surface of both materials (Fig. 5CD). Here, super-hydrophilic PANI was clearly responsible for the observed change in wettability of the conductive scaffolds [77].

3.6. Cytotoxicity assessment

To determine whether the three types of electrospun nanofiber film release cytotoxic molecules, PAN, PAN/PANI, and PAN/PANI/NI were soaked for 24 h into culture medium and then removed. The culture medium possibly contaminated with cytotoxic chemicals was then employed to cultivate rat SCs for one day. Afterward, the MTT assay was used to measure cellular metabolic activity (Fig. 6). SCs in culture media exposed to PAN, PAN/PANI, or PAN/PANI/Ni had a metabolic activity comparable to pristine medium and significantly higher than the positive cytotoxic 5% DMSO con-

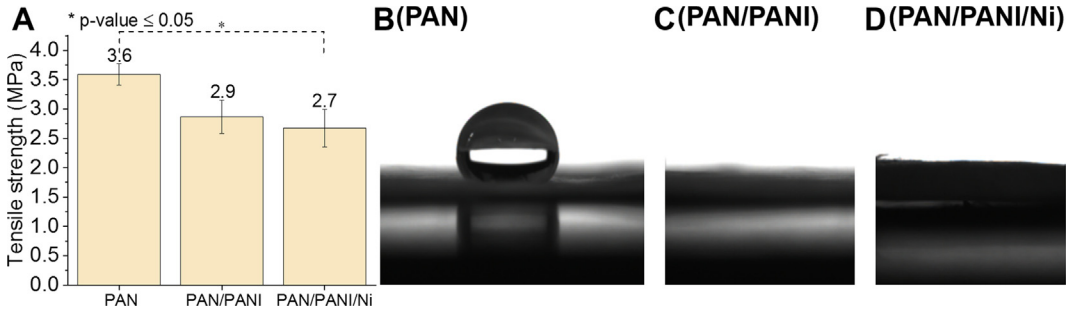

Fig. 5. Tensile strength and wettability of PAN, PAN/PANI, and PAN/PANI/Ni. (A) Tensile strength of the electrospun nanofiber films. Each bar is the mean of at least five replicates with standard deviation. Water contact angle images of (B) PAN, (C) PAN/PANI, and (D) PAN/PANI/Ni.

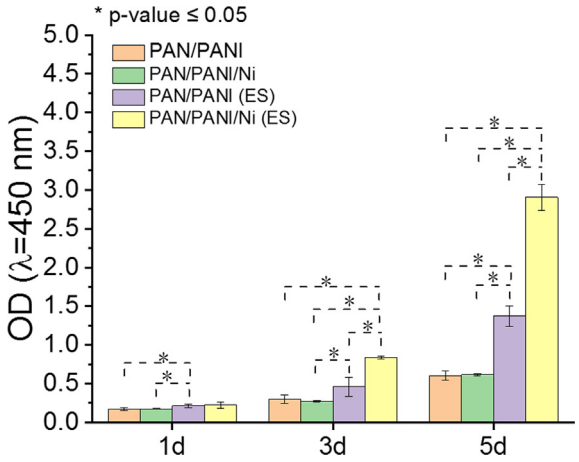

Fig. 7. Electrostimulation and SCs proliferation with PAN/PANI and PAN/PANI/Ni scaffolds. Electrostimulation was performed with a constant voltage of 100 mv cm^{-1} for one hour per day. SCs proliferation was measured with the CCK-8 assay. Each bar is the mean of at least three replicates with standard deviation. ES: electrostimulation.

trol. These results demonstrate that the three electrospun materials did not release cytotoxic molecules harmful for SCs in the culture medium and were likely to be biocompatible.

3.7. Electrical stimulation of Schwann cells proliferation

The proliferation of SCs upon electrical stimulation *via* electrically-conductive electrospun nanofiber films was quantified with the CCK-8 assay (Fig. 7). Electrical stimulation was achieved with a constant voltage of 100 mV cm^{-1} for one hour per day over a total period of five days. Without electrical stimulation, cell proliferation was similar between PAN/PANI and PAN/PANI/Ni film with higher electrical conductivity. Both PAN/PANI and PAN/PANI/Ni films exhibited faster SC proliferation after three days upon electrical stimulation. For PAN/PANI/Ni, cell proliferation increased substantially after five days with an OD_{450nm} 4.7 fold higher upon electrical stimulation than without. At 5 days, electrostimulated PAN/PANI/Ni film was also 2.1 times more efficient at promoting SC proliferation than electrostimulated PAN/PANI film demonstrating the benefit of doping with highly-conductive nickel NPs. Besides higher electrical conductivity, the lower diameter of the PAN/PANI/Ni electrospun nanofibers compared to PAN/PANI may also be involved in the faster SCs proliferation. Previous studies have shown that cell adhesion and growth was facilitated by electrospun nanofibers with a smaller diameter [78,79].

3.8. Schwann cells disposition and attachment

SEM images of electrospun films after five days of cell proliferation show the distinct shape of SCs (Fig. 8; Fig. S2). After electrostimulation, SCs were well-distributed on both PAN/PANI and PAN/

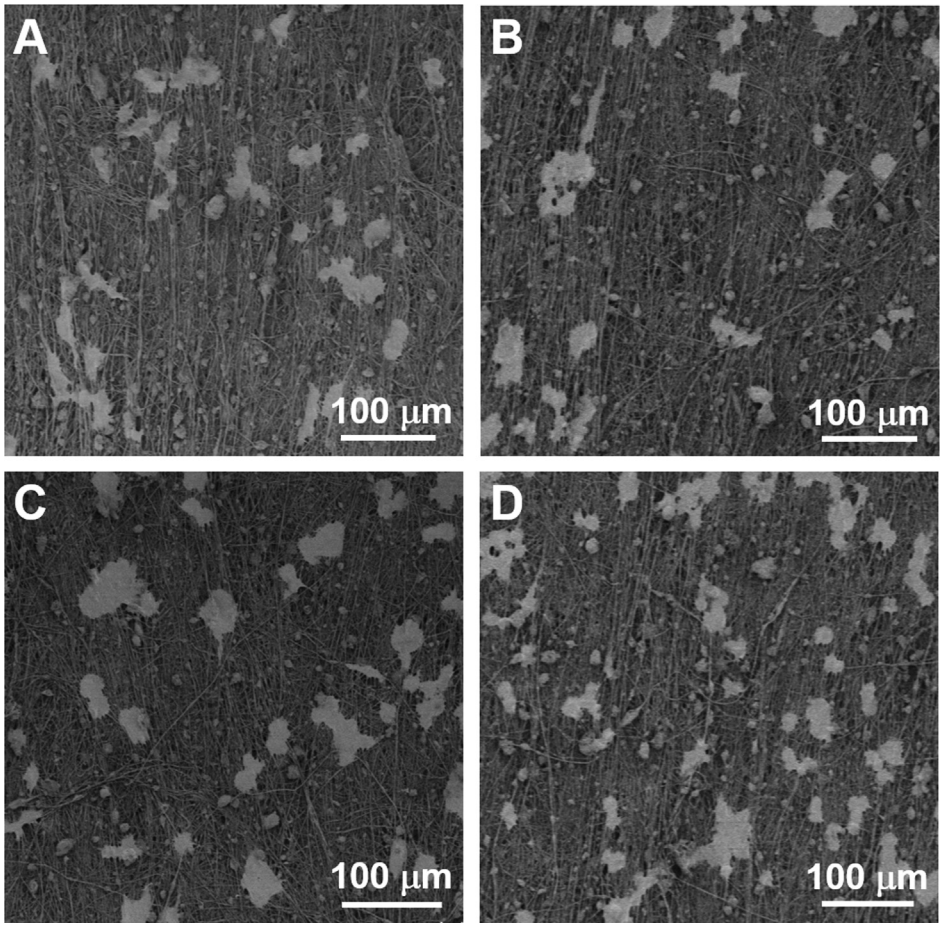

Fig. 8. SEM images after five days of SCs proliferation. (A) PAN/PANI without electrostimulation, (B) PAN/PANI/Ni without electrostimulation, (C) PAN/PANI with electrostimulation, and (D) PAN/PANI/Ni with electrostimulation.

PANI/Ni confirming the biocompatibility of these materials. Furthermore, the SEM analysis confirmed that the electrospun PAN/PANI/Ni nanofiber film was more suitable for the electrostimulation of SCs proliferation. The SEM image of PAN/PANI/Ni with electrostimulation exhibits a larger cell number than PAN/PANI with electrostimulation or PAN/PANI and PAN/PANI/Ni without electrostimulation. These results highlighted the advantage for SC proliferation of adding Ni NPs to PAN/PANI nanofibers and of increasing the electrical conductivity of the NTE scaffold.

4. Conclusions

In summary, the addition of Ni NPs to electrospun PAN/PANI nanofibers resulted in a highly-conductive and super-hydrophilic material with the proper tensile strength to serve as a scaffold for NTE. Furthermore, PAN/PANI/Ni was biocompatible for SCs with no release of cytotoxic compounds in the culture medium. Upon electrostimulation, the PAN/PANI/Ni scaffold accelerated SCs proliferation compared to PAN/PANI, which exhibited a significantly lower electrical conductivity. This observation highlights the importance of maximizing the electrical conductivity of the NTE scaffold to increase cell proliferation and possibly shorten the time required for nerve healing processes. Although the PAN/PANI/Ni biomimicking scaffold is promising additional work is required to evaluate extensively its potential for NTE. Still, the strategy proposed here to modulate the electrical properties of the electrospun PAN/PANI nanofibers with Ni NPs is straightforward and can readily be adapted for different biomimicking scaffolds developed for electrostimulation.

Declaration of Competing Interest

The authors declare that they have no known competing financial interests or personal relationships that could have appeared to influence the work reported in this paper.

Acknowledgements

This work was supported by the Chinese Thousand Talents Plan Program, Hainan Yazhou Bay Science and Technology Bureau grant No SKJC-2020-01-004, and Wuhan University of Technology.

Appendix A. Supplementary material

Supplementary data to this article can be found online at https://doi.org/10.1016/j.bioelechem.2021.107750.

References

[1] R.M.G. Menorca, T.S. Fussell, J.C. Elfar, Nerve physiology: Mechanisms of injury and recovery, Hand Clin. 29 (2013) 317–330.
[2] B.-G. Jiang, N. Han, F. Rao, Y.-L. Wang, Y.-H. Kou, P.-X. Zhang, Advance of peripheral nerve injury repair and reconstruction, Chin. Med. J. (Engl) 130 (2017) 2996–2998.
[3] A.M. Adams, K.W. VanDusen, T.Y. Kostrominova, J.P. Mertens, L.M. Larkin, Scaffoldless tissue-engineered nerve conduit promotes peripheral nerve regeneration and functional recovery after tibial nerve injury in rats, Neural Regen. Res. 12 (2017) 1529–1537.
[4] S.K. Lee, S.W. Wolfe, Peripheral nerve injury and repair, J. Am. Acad. Orthop. Surg. 8 (2000) 243–252.
[5] M.F. Meek, J.H. Coert, Clinical use of nerve conduits in peripheral-nerve repair: review of the literature, J. Reconstr. Microsurg. 18 (2002) 97–109.
[6] M.B. Chen, F. Zhang, W.C. Lineaweaver, Luminal fillers in nerve conduits for peripheral nerve repair, Ann. Plast. Surg. 57 (2006) 462–471.
[7] J. Hu, Q.-T. Zhu, X.-L. Liu, Y. Xu, J.-K. Zhu, Repair of extended peripheral nerve lesions in rhesus monkeys using acellular allogenic nerve grafts implanted with autologous mesenchymal stem cells, Exp. Neurol. 204 (2007) 658–666.
[8] A. Muheremu, Q. Ao, Past, present, and future of nerve conduits in the treatment of peripheral nerve injury, Biomed Res. Int. 2015 (2015) e237507.
[9] O. Shueibi, Z. Zhou, X. Wang, B. Yi, X. He, Y. Zhang, Effects of GO and rGO incorporated nanofibrous scaffolds on the proliferation of Schwann cells, Biomed. Phys. Eng. Express. 5 (2019) 025002.
[10] L. Yan, B. Zhao, X. Liu, X. Li, C. Zeng, H. Shi, X. Xu, T. Lin, L. Dai, Y. Liu, Aligned nanofibers from polypyrrole/graphene as electrodes for regeneration of optic nerve via electrical stimulation, ACS Appl. Mater. Interfaces. 8 (2016) 6834–6840.
[11] K. Zhang, H. Zheng, S. Liang, C. Gao, Aligned PLLA nanofibrous scaffolds coated with graphene oxide for promoting neural cell growth, Acta Biomater. 37 (2016) 131–142.
[12] J. Xie, M.R. MacEwan, A.G. Schwartz, Y. Xia, Electrospun nanofibers for neural tissue engineering, Nanoscale. 2 (2010) 35–44.
[13] M. Vivó, A. Puigdemasa, L. Casals, E. Asensio, E. Udina, X. Navarro, Immediate electrical stimulation enhances regeneration and reinnervation and modulates spinal plastic changes after sciatic nerve injury and repair, Exp. Neurol. 211 (2008) 180–193.
[14] M.P. Willand, Electrical stimulation enhances reinnervation after nerve injury, Eur. J. Transl. Myol. 25 (2015) 243–248.
[15] J.G. Hardy, R.C. Cornelison, R.C. Sukhavasi, R.J. Saballos, P. Vu, D.L. Kaplan, C.E. Schmidt, Electroactive tissue scaffolds with aligned pores as instructive platforms for biomimetic tissue engineering, Bioengineering (Basel). 2 (2015) 15–34.
[16] X. Zhou, A. Yang, Z. Huang, G. Yin, X. Pu, J. Jin, Enhancement of neurite adhesion, alignment and elongation on conductive polypyrrole-poly(lactide acid) fibers with cell-derived extracellular matrix, Colloids Surf. B Biointerfaces. 149 (2017) 217–225.
[17] R.P. Bunge, The role of the Schwann cell in trophic support and regeneration, J. Neurol. 242 (1994) S19–S21.
[18] J. Huang, Z. Ye, X. Hu, L. Lu, Z. Luo, Electrical stimulation induces calcium-dependent release of NGF from cultured Schwann cells, Glia. 58 (2010) 622–631.
[19] T. Hadlock, C. Sundback, D. Hunter, M. Cheney, J.P. Vacanti, A polymer foam conduit seeded with Schwann cells promotes guided peripheral nerve regeneration, Tissue Eng. 6 (2000) 119–127.
[20] A. Ramón-Cueto, G.W. Plant, J. Avila, M.B. Bunge, Long-distance axonal regeneration in the transected adult rat spinal cord Is promoted by olfactory ensheathing glia transplants, J. Neurosci. 18 (1998) 3803–3815.
[21] A.N. Koppes, A.L. Nordberg, G.M. Paolillo, N.M. Goodsell, H.A. Darwish, L. Zhang, D.M. Thompson, Electrical stimulation of Schwann cells promotes sustained increases in neurite outgrowth, Tissue Eng. Part A 20 (2013) 494–506.
[22] A.N. Koppes, A.M. Seggio, D.M. Thompson, Neurite outgrowth is significantly increased by the simultaneous presentation of Schwann cells and moderate exogenous electric fields, J. Neural Eng. 8 (2011) 046023.
[23] Y. Wu, L. Wang, T. Hu, P.X. Ma, B. Guo, Conductive micropatterned polyurethane films as tissue engineering scaffolds for Schwann cells and PC12 cells, J. Colloid Interface Sci. 518 (2018) 252–262.
[24] L. Forciniti, J. Ybarra, M.H. Zaman, C.E. Schmidt, Schwann cell response on polypyrrole substrates upon electrical stimulation, Acta Biomater. 10 (2014) 2423–2433.
[25] Y. Zhao, J. Gong, C. Niu, Z. Wei, J. Shi, G. Li, Y. Yang, H. Wang, A new electrospun graphene-silk fibroin composite scaffolds for guiding Schwann cells, J. Biomater. Sci. Polym. Ed. 28 (2017) 2171–2185.
[26] B. Sun, T. Wu, J. Wang, D. Li, J. Wang, Q. Gao, M.A. Bhutto, H. El-Hamshary, S.S. Al-Deyab, X. Mo, Polypyrrole-coated poly(L-lactic acid-co-ε-caprolactone)/silk fibroin nanofibrous membranes promoting neural cell proliferation and differentiation with electrical stimulation, J. Mater. Chem. B. 4 (2016) 6670–6679.
[27] H. Baniasadi, A. Ramazani S.A., S. Mashayekhan, Fabrication and characterization of conductive chitosan/gelatin-based scaffolds for nerve tissue engineering, Int. J. Biol. Macromol. 74 (2015) 360–366.
[28] J. Huang, X. Hu, L. Lu, Z. Ye, Q. Zhang, Z. Luo, Electrical regulation of Schwann cells using conductive polypyrrole/chitosan polymers, J. Biomed. Mater. Res. Part A. 93A (2010) 164–174.
[29] D. Xu, L. Fan, L. Gao, Y. Xiong, Y. Wang, Q. Ye, A. Yu, H. Dai, Y. Yin, J. Cai, L. Zhang, Micro-nanostructured polyaniline assembled in cellulose matrix via interfacial polymerization for applications in nerve regeneration, ACS Appl. Mater. Interfaces. 8 (2016) 17090–17097.
[30] L. Fan, Y. Xiong, Z. Fu, D. Xu, L. Wang, Y. Chen, H. Xia, N. Peng, S. Ye, Y. Wang, L. Zhang, Q. Ye, Polyaniline promotes peripheral nerve regeneration by enhancement of the brain-derived neurotrophic factor and ciliary neurotrophic factor expression and activation of the ERK1/2/MAPK signaling pathway, Mol. Med. Rep. 16 (2017) 7534–7540.
[31] S. Hosseinzadeh, M. Mahmoudifard, F. Mohamadyar-Toupkanlou, M. Dodel, A. Hajarizadeh, M. Adabi, M. Soleimani, The nanofibrous PAN-PANi scaffold as an efficient substrate for skeletal muscle differentiation using satellite cells, Bioprocess Biosyst. Eng. 39 (2016) 1163–1172.
[32] S. Kamalesh, P. Tan, J. Wang, T. Lee, E.-T. Kang, C.-H. Wang, Biocompatibility of electroactive polymers in tissues, J. Biomed. Mater. Res. 52 (2000) 467–478.
[33] M. Mohamadali, S. Irani, M. Soleimani, S. Hosseinzadeh, PANi/PAN copolymer as scaffolds for the muscle cell-like differentiation of mesenchymal stem cells, Polym. Adv. Technol. 28 (2017) 1078–1087.
[34] L. Wang, Q. Huang, J.-Y. Wang, Nanostructured polyaniline coating on ITO glass promotes the neurite outgrowth of PC 12 cells by electrical stimulation, Langmuir 31 (2015) 12315–12322.

[35] Y. Arteshi, A. Aghanejad, S. Davaran, Y. Omidi, Biocompatible and electroconductive polyaniline-based biomaterials for electrical stimulation, Eur. Polym. J. 108 (2018) 150–170.
[36] L. Ghasemi-Mobarakeh, M.P. Prabhakaran, M. Morshed, M.H. Nasr-Esfahani, H. Baharvand, S. Kiani, S.S. Al-Deyab, S. Ramakrishna, Application of conductive polymers, scaffolds and electrical stimulation for nerve tissue engineering, J. Tissue Eng. Regen. Med. 5 (2011) e17–e35.
[37] J. Yan, T. Wei, B. Shao, Z. Fan, W. Qian, M. Zhang, F. Wei, Preparation of a graphene nanosheet/polyaniline composite with high specific capacitance, Carbon 48 (2010) 487–493.
[38] K. Zhang, L.L. Zhang, X.S. Zhao, J. Wu, Graphene/polyaniline nanofiber composites as supercapacitor electrodes, Chem. Mater. 22 (2010) 1392–1401.
[39] X. Cai, X. Cui, L. Zu, Y. Zhang, X. Gao, H. Lian, Y. Liu, X. Wang, Ultra high electrical performance of nano nickel oxide and polyaniline composite materials, Polymers. 9 (2017) 288.
[40] L. Williams, A.R. Prasad, P. Sowmya, A. Joseph, Characterization and Temperature dependent DC conductivity study of bio templated nickel oxide nanoparticles (NiO) and their composites using polyaniline (PANI), Mater. Chem. Phys. 242 (2020) 122469.
[41] G.G. Wallace, P.R. Teasdale, G.M. Spinks, L.A.P. Kane-Maguire, P.R. Teasdale, G. M. Spinks, L.A.P. Kane-Maguire, Conductive electroactive polymers: Intelligent polymer systems, Third Edition., CRC Press, 2008.
[42] Y. Zhao, W. Zhao, S. Yu, Y. Guo, X. Gu, Y. Yang, Biocompatibility evaluation of electrospun silk fibroin nanofibrous mats with primarily cultured rat hippocampal neurons, Biomed. Mater. Eng. 23 (2013) 545–554.
[43] S.R. Bhattarai, N. Bhattarai, H.K. Yi, P.H. Hwang, D.I. Cha, H.Y. Kim, Novel biodegradable electrospun membrane: scaffold for tissue engineering, Biomaterials 25 (2004) 2595–2602.
[44] H. Liu, X. Li, G. Zhou, H. Fan, Y. Fan, Electrospun sulfated silk fibroin nanofibrous scaffolds for vascular tissue engineering, Biomaterials 32 (2011) 3784–3793.
[45] T. Li, L. Tian, S. Liao, X. Ding, S.A. Irvine, S. Ramakrishna, Fabrication, mechanical property and in vitro evaluation of poly (L-lactic acid-co-ε-caprolactone) core-shell nanofiber scaffold for tissue engineering, J. Mech. Behav. Biomed. Mater. 98 (2019) 48–57.
[46] S. Ramakrishna, K. Fujihara, W.-E. Teo, T. Yong, Z. Ma, R. Ramaseshan, Electrospun nanofibers: solving global issues, Mater. Today. 9 (2006) 40–50.
[47] I. Karbownik, O. Rac-Rumijowska, M. Fiedot-Toboła, T. Rybicki, H. Teterycz, The preparation and characterization of polyacrylonitrile-polyaniline (PAN/PANI) fibers, Materials. 12 (2019) 664.
[48] G. Zhai, Q. Fan, Y. Tang, Y. Zhang, D. Pan, Z. Qin, Conductive composite films composed of polyaniline thin layers on microporous polyacrylonitrile surfaces, Thin Solid Films 519 (2010) 169–173.
[49] N. Toptaş, M. Karakışla, M. Saçak, Conductive polyaniline/polyacrylonitrile composite fibers: Effect of synthesis parameters on polyaniline content and electrical surface resistivity, Polym. Compos. 30 (2009) 1618–1624.
[50] A. Bertea, L.R. Manea, A. Bertea, L. Hristian, Associated polymers, solvents and doping agents to make polyaniline electrospinnable, IOP Conf. Ser.: Mater. Sci. Eng. 209 (2017) 012073.
[51] J. Wang, K. Pan, E.P. Giannelis, B. Cao, Polyacrylonitrile/polyaniline core/shell nanofiber mat for removal of hexavalent chromium from aqueous solution: mechanism and applications, RSC Adv. 3 (2013) 8978–8987.
[52] H. Talbi, P.-E. Just, L.H. Dao, Electropolymerization of aniline on carbonized polyacrylonitrile aerogel electrodes: applications for supercapacitors, J. Appl. Electrochem. 33 (2003) 465–473.
[53] G. Bayramoğlu, A.Ü. Metin, B. Altıntas, M.Y. Arıca, Reversible immobilization of glucose oxidase on polyaniline grafted polyacrylonitrile conductive composite membrane, Bioresour. Technol. 101 (2010) 6881–6887.
[54] V. Mottaghitalab, G.M. Spinks, G.G. Wallace, The influence of carbon nanotubes on mechanical and electrical properties of polyaniline fibers, Synth. Met. 152 (2005) 77–80.
[55] P. Zamani, D. Higgins, F. Hassan, G. Jiang, J. Wu, S. Abureden, Z. Chen, Electrospun iron–polyaniline–polyacrylonitrile derived nanofibers as non–precious oxygen reduction reaction catalysts for PEM fuel cells, Electrochim. Acta. 139 (2014) 111–116.
[56] S. Mukherjee, S. Das, S. Nuthi, C.R. Patra, Biocompatible nickel-prussian blue@silver nanocomposites show potent antibacterial activities, Future Sci. OA. 3 (2017) FSO233.
[57] A.C.A. Silva, M.A.P. Zóia, L.I.V. Correia, F.V.P.V. Azevedo, A.T. dePaula, L.P. Maia, L.S. de Carvalho, L.N. Carvalho, M.P.C. Costa, L. CarrilhoGiaretta, R.S. Rodrigues, V. de M. Ávila, L.R. Goulart, N.O. Dantas, Biocompatibility of doped semiconductors nanocrystals and nanocomposites, cytotoxicity. (2018). https://doi.org/10.5772/intechopen.77197.
[58] K.R. Jessen, R. Mirsky, A.C. Lloyd, Schwann Cells: Development and role in nerve repair, Cold Spring Harb. Perspect. Biol. 7 (2015) a020487.
[59] W. Qi, D. Ding, R.J. Salvi, Cytotoxic effects of dimethyl sulphoxide (DMSO) on cochlear organotypic cultures, Hear Res. 236 (2008) 52–60.
[60] C. Yuan, J. Gao, J. Guo, L. Bai, C. Marshall, Z. Cai, L. Wang, M. Xiao, Dimethyl sulfoxide damages mitochondrial integrity and membrane potential in cultured astrocytes, PLoS ONE 9 (2014) e107447.
[61] L. Hao, W. Gao, S. Yan, M. Niu, G. Liu, H. Hao, Functionalized diatomite/oyster shell powder doped electrospun polyacrylonitrile submicron fiber as a high-efficiency adsorbent for removing methylene blue from aqueous solution: Thermodynamics, kinetics and isotherms, J. Mol. Liq. 298 (2020) 112022.
[62] Y. Xia, Y. Lu, Conductive polymers/polyacrylonitrile composite fibers: Fabrication and properties, Polym. Compos. 31 (2010) 340–346.
[63] T. Xu, F. Wu, Y. Gu, Y. Chen, J. Cai, W. Lu, H. Hu, Z. Zhu, W. Chen, Visible-light responsive electrospun nanofibers based on polyacrylonitrile-dispersed graphitic carbon nitride, RSC Adv. 5 (2015) 86505–86512.
[64] D. Arthisree, W. Madhuri, Optically active polymer nanocomposite composed of polyaniline, polyacrylonitrile and green-synthesized graphene quantum dot for supercapacitor application, Int. J. Hydrog. Energy. 45 (2020) 9317–9327.
[65] P. Ryšánek, O. Benada, J. Tokarský, M. Syrový, P. Čapková, J. Pavlík, Specific structure, morphology, and properties of polyacrylonitrile (PAN) membranes prepared by needleless electrospinning; Forming hollow fibers, Mater. Sci. Eng. C. 105 (2019) 110151.
[66] M.-J. Yu, Y.-J. Bai, C.-G. Wang, Y. Xu, P.-Z. Guo, A new method for the evaluation of stabilization index of polyacrylonitrile fibers, Mater. Lett. 61 (2007) 2292–2294.
[67] E.A. Sanches, J.C. Soares, A.C. Mafud, E.G.R. Fernandes, F.L. Leite, Y.P. Mascarenhas, Structural characterization of chloride salt of conducting polyaniline obtained by XRD, SAXD, SAXS and SEM, J. Mol. Struct. 1036 (2013) 121–126.
[68] Y. Ji, X. Zhang, Y. Zhu, B. Li, Y. Wang, J. Zhang, Y. Feng, Nickel nanofibers synthesized by the electrospinning method, Mater. Res. Bull. 48 (2013) 2426–2429.
[69] C. Wang, Y.-W. Cheng, C.-H. Hsu, H.-S. Chien, S.-Y. Tsou, How to manipulate the electrospinning jet with controlled properties to obtain uniform fibers with the smallest diameter?—a brief discussion of solution electrospinning process, J. Polym. Res. 18 (2011) 111–123.
[70] F.R. Lamastra, F. Nanni, L. Camilli, R. Matassa, M. Carbone, G. Gusmano, Morphology and structure of electrospun $CoFe_2O_4$/multi-wall carbon nanotubes composite nanofibers, Chem. Eng. J. 162 (2010) 430–435.
[71] J. Cheng, Y. Jun, J. Qin, S.-H. Lee, Electrospinning versus microfluidic spinning of functional fibers for biomedical applications, Biomaterials 114 (2017) 121–143.
[72] T.-K. Hung, G.-L. Chang, H.-S. Lin, F.R. Walter, L. Bunegin, Stress-strain relationship of the spinal cord of anesthetized cats, J. Biomech. 14 (1981) 269–276.
[73] G.H. Borschel, K.F. Kia, W.M. Kuzon, R.G. Dennis, Mechanical properties of acellular peripheral nerve, J. Surg. Res. 114 (2003) 133–139.
[74] C.H. Kim, M.S. Khil, H.Y. Kim, H.U. Lee, K.Y. Jahng, An improved hydrophilicity via electrospinning for enhanced cell attachment and proliferation, J. Biomed. Mater. Res. Part B Appl. Biomater. 78B (2006) 283–290.
[75] D.M. Correia, C. Ribeiro, G. Botelho, J. Borges, C. Lopes, F. Vaz, S.A.C. Carabineiro, A.V. Machado, S. Lanceros-Méndez, Superhydrophilic poly(l-lactic acid) electrospun membranes for biomedical applications obtained by argon and oxygen plasma treatment, Appl. Surf. Sci. 371 (2016) 74–82.
[76] G. Li, Q. Xiao, L. Zhang, Y. Zhao, Y. Yang, Nerve growth factor loaded heparin/chitosan scaffolds for accelerating peripheral nerve regeneration, Carbohydr. Polym. 171 (2017) 39–49.
[77] G.R. Guillen, T.P. Farrell, R.B. Kaner, E.M.V. Hoek, Pore-structure, hydrophilicity, and particle filtration characteristics of polyaniline–polysulfone ultrafiltration membranes, J. Mater. Chem. 20 (2010) 4621–4628.
[78] M. Chen, P.K. Patra, S.B. Warner, S. Bhowmick, Role of fiber diameter in adhesion and proliferation of NIH 3T3 fibroblast on electrospun polycaprolactone scaffolds, Tissue Eng. 13 (2007) 579–587.
[79] G.T. Christopherson, H. Song, H.-Q. Mao, The influence of fiber diameter of electrospun substrates on neural stem cell differentiation and proliferation, Biomaterials 30 (2009) 556–564.